Numerical Determination of the Optimal Design Parameters for a Phased Array Based Ultrasonic Polar Scan

Jannes Daemen, Arvid Martens, Mathias Kersemans, Erik Verboven, Steven Delrue, Wim Van Paepegem, Koen Van Den Abeele

***Abstract*—In the context of a next-generation Ultrasonic Polar Scan (UPS) measurement system, this research aims to look at the possibility to use a set of cylindrically focused emitters in conjunction with a Circular Phased Array (C-PA) receiver in order to create a portable measurement system, while improving the data quality. To do so, an three-dimensional analytical model is presented to simulate UPS experiments with the proposed system. In addition, a post-processing procedure is worked out to treat the acquired raw data with the aim to reconstruct the angle dependent plane wave reflection coefficients of the sample under study. As this reconstruction will depend heavily on various design parameters, three parameter studies are performed to find the optimal design. First, it the radius of the C-PA and the used frequency are varied, and it is shown that given a particular frequency, the radius must be large enough to capture the full reflected field such that an accurate reconstruction of the plane wave characteristics can be performed. Second, the emitter and receiver widths are varied and it is shown that by increasing either of them, better results can be achieved. However, in order to get the best results, both widths should be considerably large. Third, the pitch and the angular range of the cylindrically focused emitters are varied, and it is shown that if the pitch is too large, aliasing effects will disturb the results. However, this effect can somewhat be mitigated by using multiple emitters with a restricted angular range. Using the knowledge of the previous parameter studies, a simulated UPS experiment using a good set of design paramters is performed for a cross-ply Carbon Epoxy laminate which shows an excellent agreement with the theoretical plane wave results.**

***Index Terms*—Ultrasonic Polar Scan, Phased Array, Composite materials, Nondestructive testing**

I. Introduction

A multitude of accurate and reliable non-destructive experimental techniques exist with the aim to determine the (visco-)elastic properties of materials. However, rather than providing insight on the full viscoelastic tensor, it can typically only partially be determined. The Ultrasonic Polar Scan (UPS) is a state-of-the-art technique which aims to determine the full viscoelastic C-tensor of materials [1], [2], [3], [4], while also offering the possibility to assess damage within structures [5], [6], [7]. During an UPS measurement, as seen in Fig. 1a, an ultrasonic transducer emits a broadband signal from multiple oblique incidence angle $\Psi(\theta_s, \phi_s)$ on the hemisphere. After interaction with the plate under study, either the reflected or transmitted signals are captured by a second transducer, after which these data are used to determine the angle dependent reflection or transmission coefficients, or the Time-Of-Flight (TOF). These results can be summarized in polar plots such that characteristic shapes appear which essentially provide a local fingerprint of the material [8]. As an example, Fig. 1b shows the experimentally determined transmission coefficient of an 1.4 mm thick $[0,90]_S$ cross-ply Carbon/Epoxy plate. Due to the one-to-one relationship between the C-tensor and the polar plot data by virtue of the Christoffel equations, it is possible to use the data in an plane wave based inversion algorithm to uniquely determine the viscoelastic properties of the material [9], [2], [3], [8]. Alternatively, in order to provide insight into the frequency dependence of the viscoelastic tensor, the measured signals can be analyzed in a spectroscopic manner by transforming the data to the frequency domain [10].

Even though excellent experimental results were achieved by an in-house built five-axis UPS setup, it was found that it would be too inconvenient to use in an industrial setting. Indeed, the measurement duration is relatively long due to the mechanical positioning of the emitter-receiver pair, and the need to water immerse the system to ensure a good acoustic coupling denies the possibility to perform in-field measurements. Moreover, as the transducers are finite in size, the measured data are be influenced by bounded beam effects, especially for harmonic input signals, such that the use of a plane wave model to invert the data is not strictly valid. Therefore, it is proposed to use a set of cylindrically focused transducers which are fixed on an arc in conjunction with a (semi-) Circular Phased Array (C-PA), as illustrated in Fig. 2. In this design, the cylindrically focused transducers act as a set of emitters which generate broadband signals with a large angular content, i.e. composed of multiple plane waves with different angles of incidence, whereas the C-PA is used to receive the reflected signals. Together with the large receiving aperture size of the C-PA, this to acquire information on the full wavefield composed of multiple plane wave components at once, speeding up the measurement process considerably and increasing the amount of data which can be used during the analysis of the plate properties. Appropriate post-processing

Manuscript received ***; ***

Support from the Fund for Scientific Research-Flanders (FWO Vlaanderen, grant G0B9515N, 1S45216N and 12T5418N), and the NVIDIA corporation is gratefully acknowledged.

J. Daemen, A. Martens, S. Delrue and K. Van Den Abeele are with the Department of Physics, KU Leuven Kulak, Belgium, e-mail: jannes.daemen@kuleuven.be.

M. Kersemans, E. Verboven and W. Van Paepegem are with the Department of Materials, Textiles and Chemical Engineering, Ghent University, Belgium.

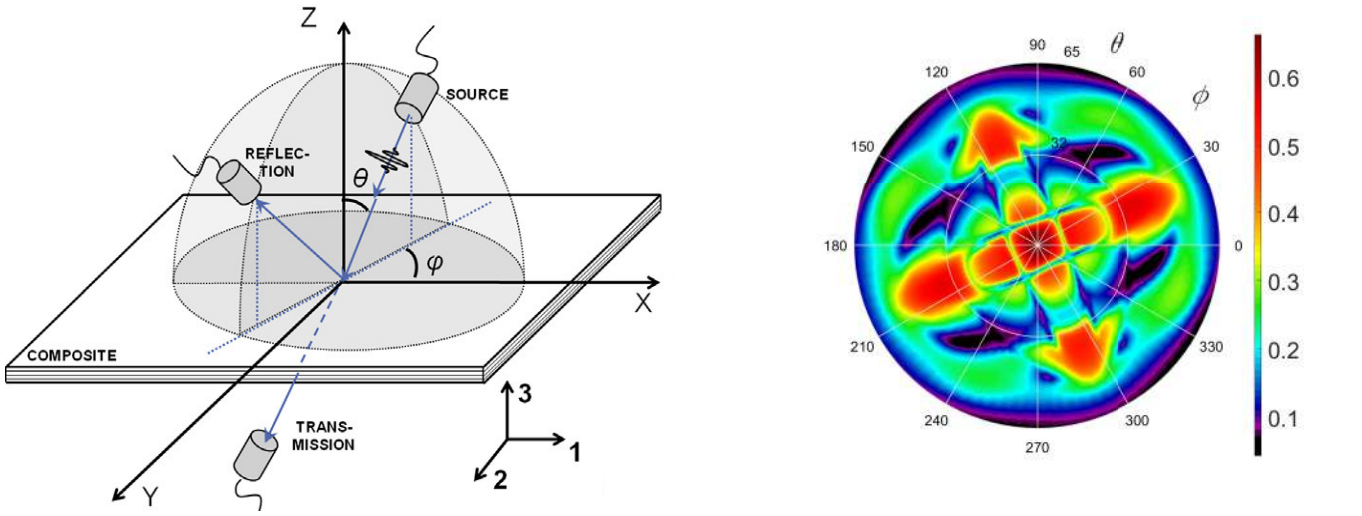

(a) (b)

Fig. 1. Schematic showing the principle of a UPS measurement (a). The plate is scanned in a rotational manner using a pair of emitting and receiving transducers. Using this method, the transmitted amplitude can for instance be measured and visualized in a polar plot (b). This result corresponds to a 1.4 mm thick $[0,90]_S$ cross-ply carbon/epoxy laminate and a broadband pulse with a center frequency of 4 MHz was used. The cross that is apparent in the polar plot can be associated to the cross-ply nature of the sample.

strategies can then be used to determine the plane wave reflection coefficients for the individual plane waves. In order to select different incident polar angles, the arc with the acoustic elements can be rotated around a central axis, i.e. the z-axis on Fig. 2, such that only a single mechanical movement is needed. The whole system would be placed in a dome-like structure and be filled with water which is kept inside by using a thin membrane at the bottom of the structure to ensure a good acoustic coupling between the transducers and the plate, reminiscent to the use of a water bag [11].

In previous work, it was already shown via 2D simulations that the concept of using a C-PA can work along the main axes of orthotropy of a material [12]. However, in order to determine the full viscoelastic C-tensor, measurement data related to different polar angles are also needed, and unfortunately these incident angles could not be investigated with the 2D model. Indeed, along these incident angles, the reflected field may partially be skewed in a direction different from the incident polar angle, which is a genuine 3D effect. In addition to the limited applicability of the 2D simulations, they were also rather slow such that an extensive parameter study on the optimal design parameters of the device could not be performed. Therefore, it is the aim of this study to adapt and extend the 2D model to a faster 3D version to simulate UPS experiments along all polar angles. Based on this enhanced model, a parameter study is done to optimize the design such that the simulated measurement data correspond to plane wave results as close as possible, making the subsequent plane wave based inversion of the data easier. This optimization is performed as a function of the various design parameters such as the (i) the radius the C-PA, (ii) the depth of the C-PA receivers and the emitters, and (iii) the pitch of the receivers, and the number of emitters. Eventually, after finding a suitable set of values for the various design parameters, they are reused to show that this kind of measurement device can also be used for more complex composites, such as a cross-ply Carbon/Epoxy plate.

II. Simulation Model and Data Analysis

While the 2D simulations reported in previous work were conducted using FEM [12], full 3D FEM simulations of the proposed design proved to be too computationally expensive to perform. Therefore, it was opted to build an analytical model, also shown in Fig. 2, in which the incident pulses are calculated by FOCUS [13], [14] and the interaction with the plate is based on known theoretical models using the Christoffel equations and the partial wave technique [9]. The propagation of the wave fields is done by applying Discrete Fourier Transforms and appropriate phase shifts based on the travel path. In this model, the number of emitting cylindrically focused transducers can be varied, as well as their angular range Θ and depth l_e. The number of receiving array elements can also be varied, as well as their pitch and depth l_r. Furthermore, the array elements can be positioned in either a single circular configuration, or bundled in several linear arrays such that he circular configuration is approximated.

A. Simulation of the reflected fields

As a first step, the incident complex pressure fields generated by the multiple emitting cylindrically focused transducers are calculated by FOCUS individually. These fields are calculated in the frequency domain for specific frequencies f such that any pulse can be reconstructed by using appropriate weights and an Inverse Fast Fourier Transform (IFFT). In the following, the field experienced by the plate generated by the i^{th} emitter for a particular frequency f will be denoted as $p_f^i(x,y)$ where x and y are coordinates on the plate surface with respect to a coordinate system rotated by the incident

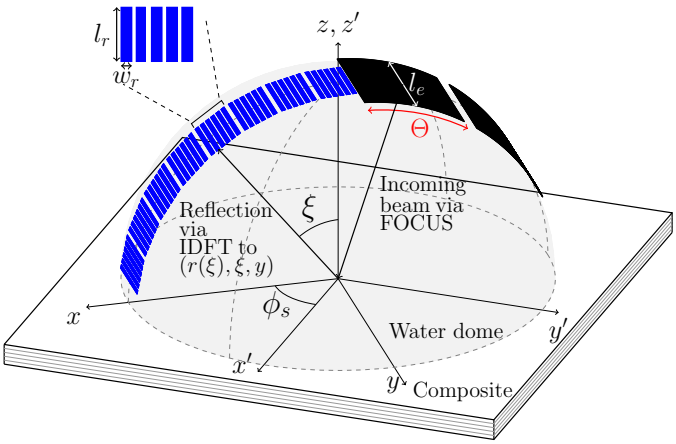

Fig. 2. Schematic representation of the new C-PA based system. One or multiple transducers with an angular range Θ are used to generate focused beams containing many plane wave components. The reflected field is then measured by the Phased Array elements. In the simulation model, the dimensions of the array and the emitters can be changed, as well as the specific positioning of the array elements, i.e. along an arc or bundled in multiple linear sub-arrays, and the number of emitters.

angle ϕ_s. Evidently, the incident beam is comprised of multiple plane wave components, meaning that since the Christoffel equations are only defined for plane waves, the fields $p_f^i(x, y)$ have to be spatially decomposed in a plane wave spectrum, namely

$$I_f^i(k_x, k_y) = \sum_{x,y} p_f^i(x, y) e^{i(k_x x + k_y y)}. \tag{1}$$

In this equation k_x and k_y denote the wave vector components in the x and y direction such that $k_z = \sqrt{k^2 - k_x^2 - k_y^2}$ and $k = \frac{2\pi f}{v}$, where v is the speed of sound in the fluid surrounding the plate. In order to take into account the plate interaction, $I_f^i(k_x, k_y)$ has to be multiplied by plane wave reflection coefficients $R_f(k_x, k_y)$, which are calculated through the Christoffel Equations. This multiplication then results in the plane wave components of the reflected field at plate surface, and can be used to construct the reflected field at the location of the PA elements. Even though the PA elements might be small in size, the reflected field will still vary across their apertures such that an integration of the fields experienced by each individual PA element is needed. To do so, these apertures are discretized by evaluating the reflected field on multiple points across the aperture, after which those points are summed together such that a single pressure value is found for each PA element. Due to the (quasi-) circular arrangement of the PA elements, it is most convenient do describe these discretized positions in cylindrical coordinates, i.e. as a function of the angle ξ, the radius $r(\xi)$ and their lateral positions along the y-axis y. As such the reflected pressure as a function of ξ, $r(\xi)$ and y is written as

$$P_f^i(r(\xi), \xi, y) = \sum_{k_x, k_y} I_f^i(k_x, k_y) R_f(k_x, k_y) e^{-i\alpha(k_x, k_y, r(\xi), \xi, y)}. \tag{2}$$

This equation describes a Inverse Discrete Fourier Transform (IDFT) in which the reflected plane wave components $I_f^i(k_x, k_y) R_f(k_x, k_y)$ are multiplied by a phase shift to account for the propagation of the plane waves towards the array. The phase shift can be calculated purely from geometrical considerations as

$$\alpha(k_x, k_y, r(\xi), \xi, y) = r(\xi)(\sin(\xi)k_x + \cos(\xi)k_z) + y k_y. \tag{3}$$

After summation over the points discretizing the elements, the pressure experienced by the j^{th} element is given by

$$\tilde{P}_f^{i,j} = \sum_{\xi, y} P_f^i((r(\xi), \xi, y)), \tag{4}$$

where ξ and y only take into account points related to the relevant PA element. In the following, it will be more convenient to identify the PA elements by their positions, rather than by their index j. To do so, the pressure measured across all elements can be written as $\tilde{P}_f^i(r(\zeta), \zeta)$, where the points $(r(\zeta), \zeta)$ correspond to the central positions of the PA elements in cylindrical coordinates. Note that y is implicitly assumed taken to be zero as the PA centers follow the x-axis.

In order to properly post-process the data, a reference reflected field $\tilde{P}_{f,\text{ref}}^i(r(\zeta), \zeta)$ also needs to be determined. To do so in the simulation, the reflection coefficients $R_f(k_x, k_y)$ need to be set to unity in Eq. (2), corresponding to a perfect reflector. The fields experienced by the PA elements $\tilde{P}_f^i(r(\zeta), \zeta)$ and $\tilde{P}_{f,\text{ref}}^i(r(\zeta), \zeta)$ can be considered as a set of virtual data that mimic the experimental data. The described process can be repeated for various incident angles ϕ_s to calculate the reflected fields for the whole set of incidence angles $\Psi(\theta_s, \phi_s)$, or for multiple frequencies to check their frequency dependence.

B. Calculation of the plane wave reflection coefficients

In order to determine how the simulated (or experimental) data captured by the C-PA elements should be post-processed in order to find the plane wave reflection coefficients, it is instructive to reconsider Eq. (2). Indeed, this equation describes an IDFT in which the reflection coefficient is used, which suggests that the pressure data can be used to back-calculate the plane wave reflection coefficients as a function of k_x through a DFT. However, in the context of UPS, it is more natural to describe the reflection coefficients as a function of the incident angle θ_s, for which holds that $\sin^{-1}(k_x/k) = \theta_s$. The plane wave components of the actual and the reference reflected fields at the location of the plate can then be calculated as

$$G_{f(,ref)}^i(\theta_s) = \sum_{\zeta} r(\zeta) \tilde{P}_{f(,ref)}^i(r(\zeta), \zeta) e^{i\alpha(\theta_s, r(\zeta), \zeta)} \tag{5}$$

$$= \tilde{I}_f^i(\theta_s) \tilde{R}_{f(,ref)}^i(\theta_s), \tag{6}$$

where $\alpha(k_x, r(\zeta), \zeta) = r(\zeta)(\sin(\zeta) + \cos(\zeta))$, and $\tilde{R}_{f,ref}^i(\theta_s)$ is unity. The additional factor $r(\zeta)$ in the summation is due to the transformation from a cylindrical coordinate system to a rectangular coordinate system to properly compute the DFT. From Eqs. (5) and (6), the reflection coefficient can finally be found as

$$\frac{G_f^i(\theta_s)}{G_{f,ref}^i(\theta_s)} = \tilde{R}_f^i(\theta_s) \approx R_f^i(\theta_s), \tag{7}$$

TABLE I
BASE DESIGN PARAMETERS USED IN THIS STUDY. AT MOST TWO OF THESE ARE VARIED IN EACH SIMULATION SERIES.

Radius*	100 mm
# Elements	426 (positioned between 0° and -80°)
Element width	0.3 mm
Pitch***	0.35 mm
Element depth**	2 mm
# Emitters***	2 (@ 15° and 30°)
Emitter angular range***	30°
Emitter depth**	80 mm

* Varied in subsection III-A.
** Varied in subsection III-B.
*** Varied in subsection III-C.

where it should be stressed that $\tilde{R}_f^i(\theta_s)$ is only an approximation of the exact plane wave reflection coefficient $R_f^i(\theta_s)$. Indeed, the quality of this approximation depends entirely on the discretization of the reflected field that is used in the DFT. As such, several system parameters will directly influence the final results, such as the pitch, the aperture size of the individual elements and the corresponding integration with respect to this aperture, the overall radius of the system which influences to total receiving aperture, etc.

III. RESULTS

In order to determine the optimal design parameters of the proposed phased array based UPS device, multiple parameters studies have been performed. Specifically, the impact on the result for three important sets of parameters will be discussed, which are (i) the radius R of the C-PA and the used frequency, (ii) the combined effect of the depth of the array elements l_r and the depth of the cylindrically focused emitters l_e, and (iii) the combined effect of pitch of the receivers, and the number of emitters and their angular ranges Θ. For each series of simulations, a base design is assumed such that only one or two (coupled) parameters are varied at the same time. These base parameters can be seen in Table I. In each of the cases, a unidirectional Carbon/Epoxy plate of thickness d = 1.25 mm is considered, characterized by the C-tensor given in Table II. Unless stated otherwise, full polar scans have been simulated, i.e. incident angles $\Psi(\theta_s, \phi_s)$ with $\theta_s \in [0°, 60°]$ and $\phi_s \in [0°, 360°[$ were used. This way, the anisotropic character that is inherent to the plate is fully considered in the study.

A. Radius dependence

In a first parametric study, the frequency is varied between 1 and 5 MHz and the influence of the radius on the results is investigated. To illustrate the impact of changing the radius, the reflection coefficient for a particular ϕ_s angle can be considered, for instance $\phi_s = 20°$. This is shown in Fig. 3 for both a C-PA with a radius of 0.03 m and for 0.1 m, together with the comparison to the theoretical plane wave results, using an harmonic signal of 2 MHz. While it is clear that for θ_s values above 20° there is a resonable agreement between the theoretical and simulated reflection coefficients if the radius is 0.03 m, large discrepancies can be observed for lower incident angles such that the first expected minima cannot even be distinguished. In contrast, if a larger radius

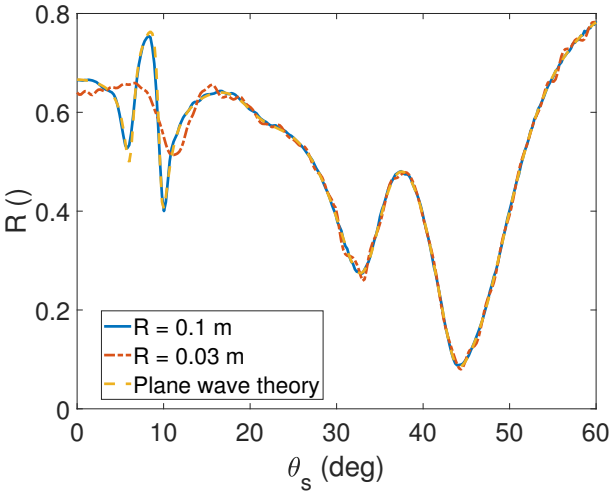

Fig. 3. Plot showing a comparison between the results obtained by using a C-PA with either a radius of 0.03 m or 0.1 m, and the theoretically expected result. The used frequency is 2 MHz and the incident polar angle ϕ_s is 20°.

is used, the agreement between the simulated results and the plane wave results becomes considerably better, even though small differences can be still be observed. This suggests that using a larger radius is beneficial for the measurement, even though this impacts the portability of the system. To understand this effect, one can consider the spatial extend of the reflected field, consisting of a direct, specular component and an indirect, non-specular component which is due to guided waves travelling through the plate and leaking into the surrounding water. Indeed, the leakage can be quite extensive such that part of this field may not be captured by the C-PA if its radius is too small [12]. This results in a loss of information, due to which the DFT-based post-processing procedure used to retrieve the reflection coefficients cannot be performed properly.

Figure 4 shows the Root Mean Squared Error (RMSE) between the reconstructed and theoretical plane wave results for various radii of the C-PA and several frequencies. Note that the RMSE from a linear scale to a dB scale using the following equation:

$$\text{RMSE}_{\text{dB}} = 10\log_{10}(\text{RMSE}_{\text{linear}}/10^{-3}). \tag{8}$$

As expected from the reasoning above, the RMSE becomes smaller once the radius increases as the reflected field can be more appropriately captured. Additionally, it is clear that for higher frequencies, the RMSE also generally lowers for a fixed radius. This effect can be attributed to the fact that not only the guided waves travelling through the plate will leak their energy into the surrounding fluid more easily, but also that these guided waves will be more strongly damped at higher frequencies.

B. Influence of the element and emitter depth

Even though the incident angles ϕ_s define a single measurement plane, the reflected field is not strictly limited to this plane, but rather extends itself in other directions as well.

TABLE II
VISCOELASTIC PARAMETERS OF THE UNIDIRECTIONAL CARBON EPOXY LAYERS USED IN THIS STUDY. THE C-TENSOR IS IN GENERAL COMPLEX AND DENOTED AS $C_{ij} = \mathcal{R}(C_{ij}) - i\mathcal{I}(C_{ij})$, WHERE i IS THE COMPLEX NUMBER.

	Viscoelastic Parameters (GPa)								
	C_{11}	C_{12}	C_{13}	C_{22}	C_{23}	C_{33}	C_{44}	C_{55}	C_{66}
$\mathcal{R}(C)$	122.73	6.5664	6.5664	13.465	6.5542	13.465	3.3980	5.8600	6.2500
$\mathcal{I}(C)$	8.5909	0.4596	0.4596	0.9426	0.4588	0.9426	0.2379	0.4102	0.4375

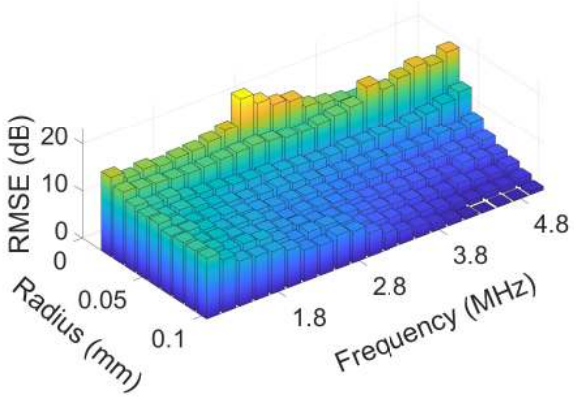

Fig. 4. Bar chart showing the RMSE (normalized such that 0 dB = 0.001) between the simulated UPS and theoretical Plane Wave results for various frequencies and radii.

Hence, the depth of the array elements, i.e. the dimension of the element along the y-direction in Fig. 2, will determine to what extend the reflected field will be captured, and thus influence to what extend proper plane wave results can be retrieved. Additionally, as the shape of the emitter will influence the input signal, and hence the reflected signals, variations of the emitter depth will indirectly influence the fields captured by the C-PA, and thus also the plane wave reconstruction. Note that these effects will be more important for measurement planes which do not align with the symmetry axes of the material. Indeed, in that case guided waves will travel through the plate and leak their energy in directions different from the measurement plane. As such, capturing a sufficient amount of the reflected field will become more difficult if receivers with a small depth are used.

To illustrate this, simulation results are shown in Fig. 5 for two different array element depths, namely 1.5 mm and 10 mm, and assuming a emitter depth of 30 mm. Even though the general trend of the reflection coefficient is found if the element depth is 1.5 mm, discrepancies with respect to plane wave results can be seen. This is most apparent below $\theta_s = 10°$, where the local extrema have shifted slightly compared to their expected location. If the depth is increased to 10 mm, the local extrema are no longer shifted from their expected location, leading to better overall match between the simulated result and the plane wave result, even though the extrema are still slightly over- or underestimated. This result suggests that the use of elements that are able to capture a considerable fraction the reflected field located outside the measurement plane, is beneficial, and can be explained by the fact that bounded beam effects, i.e. the beam is composed of multiple (non-zero) k_y components, are present when an emitter of finite size is used. Based on the principle of reciprocity, the bounded beam effects can only be filtered out if the receiver is considerably large [15], [16].

Given that the bounded beam nature of the incident beam causes problems in the reconstruction of the plane wave reflection coefficients, it should also be possible to improve the results by using an emitter with a larger depth. Indeed, in that case the incident beam will approximate a plane wave better in the y-direction, meaning that the non-zero k_y components will be less prominent, as well as guided waves which propagate in a skewed direction through the plate. Therefore, the bounded beam effects can be more easily easily filtered out by the receiver aperture. The purple curve seen in Fig. 5 corresponds to a calculation of the reflection coefficient where a receiver depth of only 1 mm is used, whereas the emitter depth was 80 mm, and shows that the result can indeed be improved by using a large emitter depth.

Fig. 6 shows the RMSE (Eq. (8)) as a function of the element and emitter depths. In agreement with the results discussed in Fig. 5, the RMSE has the tendency to go down if the emitter width or receiver widths are increased, until the improvement saturates due to other design considerations such as the radius dependence discussed earlier. Note that if a large receiver is used, the error remains considerably large if the emitter width is small, suggesting that using both a large emitter and a large receiver is essential to the design of the system in order to get good results.

C. Dependence on the pitch and the angular range of the emitter

As the determination of the plane waver reflection coefficients is based on Fourier transforms, it is evident that the reflected field has to be discretized densely enough in order to avoid aliasing effects. In this application, the discretization of the field itself is fully determined by the pitch, but the aliasing effect may be different for each individual reconstructed plane wave. Indeed, due to the curved nature of the array, a particular plane wave component may be sufficiently discretized by a part of the array where its incidence is near perpendicular to the array surface, but at the same time insufficiently discretized where the incidence is rather oblique. Therefore, some parts of the array may measure data which are aliased such that the reflection coefficient of the plane wave components incident perpendicularly to these parts of the array, are distorted.

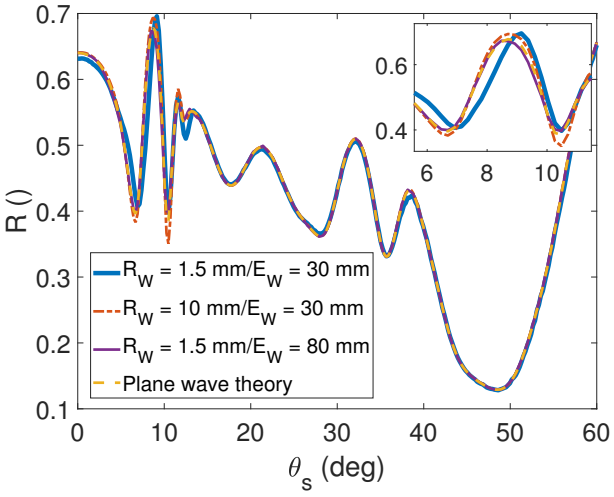

Fig. 5. Plot comparing the results achieved when both the lateral width of the receiver and emitter are relatively small, i.e. 1.5 mm and 30 mm, when the lateral width of the receiver is increased to 10 mm, and when the lateral width of the emitter is increased to 80 mm. The used frequency is 4 MHz and the incident polar angle ϕ_s is 40°. The inset shows a zoom of the results for incident angles θ_s between 6° and 11°.

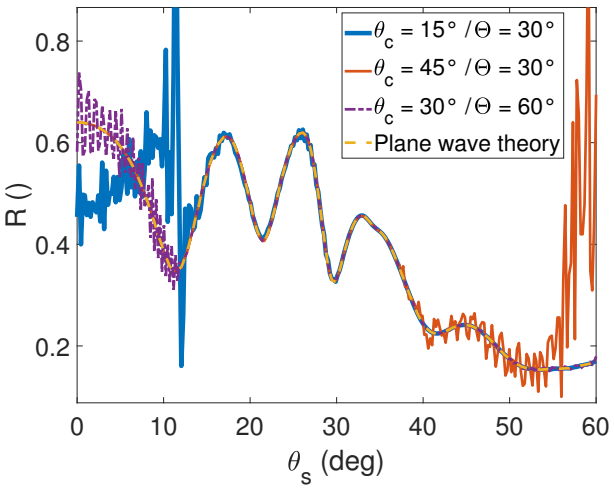

Fig. 7. Plot showing the result obtained for a C-PA with either a single emitter with an angular range of 60°or two emitters with an angular range of 30°, positioned at 15°and 45°. Merging the latter two curves at $\theta_s = 30°$allows to reconstruct the result for the full range of $\Theta = 60°$. The used frequency is 4 MHz and the incident polar angle ϕ_s is 75°.

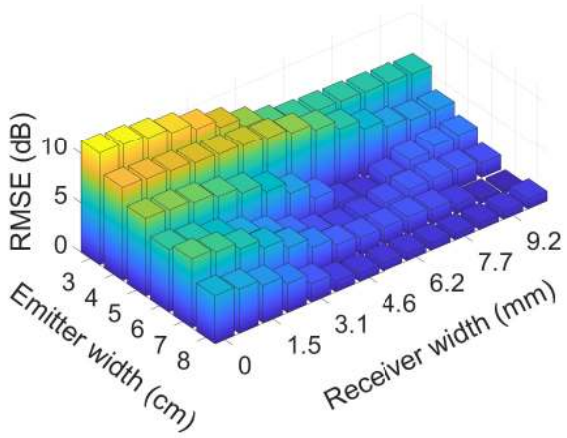

Fig. 6. Plot showing the RMSE of the simulated results with respect to the theoretical plane wave results for various emitter and phased array element depths.

This effect is illustrated in Fig. 7. The purple curve shows the result obtained when a single emitter with a large angular range of 60° is used. In this case, the plane wave components corresponding to incident θ_s angles near 60° will not be sufficiently discretized by the array elements located at low ζ values. This results in a distortion of the collected data in this region such that the reflection coefficient of the plane wave components corresponding to θ_s angles between 0° and 10° can not be reconstructed correctly. While using a smaller pitch would resolve the problem, this would make the system more complex and costly. Another option is to use multiple emitters with smaller angular ranges Θ, perform a measurement for each emitter, and treat the data independently such that plane wave components corresponding to large θ_s values do no longer interfere with the components corresponding to low θ_s values, and vice versa. Afterwards, the multiple results can be merged together to retrieve the reflection coefficient across the whole angular space. Fig. 7 shows the unmerged results for two different emitters with $\Theta = 30°$ and illustrates that even tough the data of the first emitter can only accurately retrieve the reflection coefficient up to $\theta_s = 40°$, the second emitter can provide the information for the remaining higher angles.

Fig. 8 shows the obtained RMSE for different pitch sizes and number of emitters for a simulation at 4 MHz. As expected, the RMSE generally goes downs with decreasing pitch as the aliasing effects become less severe. Similarly, a decrease in RMSE is typically also observed for an increasing number of emitters, even though this decrease is rather slow if the pitch becomes large with respect to the wavelength. If the pitch becomes sufficiently small, using a single emitter clearly does not yield good results, but the results improve drastically once more emitters are used. However, for small pitches the decrease in RMSE becomes only marginally smaller and might even slighly increase once three or more emitters are used, meaning that the plane wave content of the individual emitters has become sufficiently small to rule out aliasing effects at the used frequency.

D. Simulation of a cross-play laminate

The previous results have shown that it may be possible to find a suitable set of design parameters to perfom accurate UPS measurements with the aim of obtaining plane wave results. However, these results are all based on a single particular case, namely a unidirectional Carbon/Epoxy plate. As other types of laminates are also used in the industry, it is interesting to check whether the obtained results hold if a more complex plate is assumed. Using the knowledge acquired in the parameter

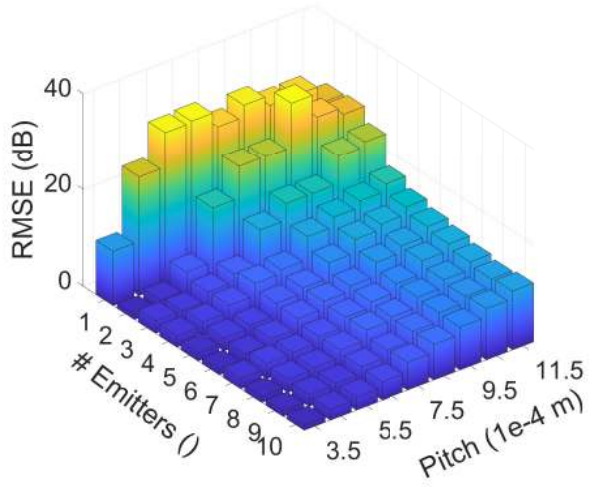

Fig. 8. Plot of the RMSE of the simulated results with respect to the theoretical plane wave results as a function of the pitch and the number of emitters. The total angular range of the emitter is 60° such that each individual emitter covers an equal fraction of this total range.

TABLE III
DESIGN PARAMETERS USED FOR THE SIMULATION OF A FULL UPS POLAR SCAN OF THE CROSS-PLY LAMINATE.

Radius	100 mm
# Elements	426 (positioned between 0° and -80°)
Element width	0.3 mm
Pitch	0.35 mm
Element depth	10 mm
# Emitters	4 (@ 7.5°, 22.5°, 37.5° and 52.5°)
Emitter angular range	15°
Emitter depth	70 mm

studies, it was reasoned that for a numerical experiment with a frequency of 4.5 MHz of a cross-ply laminate of 1.25 mm with a $[0_2 90_2]_{2S}$ layup, the design parameters presented in Table III should be sufficient.

Fig. 9a shows the reflection coefficient polar plot for the cross-ply laminate. As expected, cross-like patterns can be observed which visually identify the type of layup. Fig. 9b shows the difference between the simulated result and the theoretical plane wave results. It is clear that overall, there is a very good agreement between the two results as the errors are mostly lower than 0.001 and the total RMSE is -0.88 dB. Only near the center, a cross-like shape is visible where the absolute errors increase slightly to a maximum of 0.008, likely due to sharper features with rather extended non-specular field components which could not be completely captured using the proposed design parameters. This shows that even though the design parameters were optimized for a particular case, one can still expect good results for more involved structures.

IV. CONCLUSION

This paper presented 3D simulation results of UPS experiments on composite materials with the aim to define the design parameters for a Phased Array based Ultrasonic Polar Scan system which may serve as a portable alternative to the current experimental setup. A simulation procedure was presented for which a set of cylindrically focused transducers can be used as emitters, a Circular Phased Array which is used as the receiver, and in which Discrete Fourier Transforms are used to treat the propagation of the reflected fields. The post-processing of the generated UPS data is also based on the use of Discrete Fourier Transforms and was shown to be a reliable strategy to determine the plane wave reflection coefficients of the plate for various incident angles, if the device is properly designed. Three sets of design parameters were discussed in more detail.

- First, it was shown that for a given frequency, the error decreases with an increasing radius. However, the error also decreased with increasing frequency, making the radius requirements less stringent for higher frequencies, which benefits the envisioned portability of the system.
- Second, it was shown that the result improved when either the depth of the array elements, or the emitters is increased. However, in order to attain the best results, both should be optimized at the same time.
- Third, it was shown that the use of a small pitch is very important to avoid aliasing effect that disrupt the data quality. However, it was also shown that these issues can to some extend be circumvented by using multiple emitters with smaller angular ranges.

Using the information provided by these three parameter studies, a set of design parameters could be chosen which should yield good results. Subsequently, they were used to simulate an UPS experiment on a cross-ply Carbon/Epoxy laminate and it was shown that the RMSE can be as low as -0.88 dB, meaning that indeed a very good agreement with the theoretical plane wave results can be found.

REFERENCES

[1] M. Van Dreumel, "Nondestructive composite laminate characterization by means of ultrasonic polar-scan," *Materials Evaluation*, vol. 39, pp. 922–925, 1981.

[2] M. Kersemans, A. Martens, J. Degrieck, K. Van Den Abeele, S. Delrue, L. Pyl, F. Zastavnik, H. Sol, and W. Van Paepegem, "The Ultrasonic Polar Scan for Composite Characterization and Damage Assessment: Past, Present and Future," *Applied Sciences*, vol. 6, no. 2, p. 58, Feb. 2016.

[3] A. Martens, M. Kersemans, J. Daemen, E. Verboven, W. Van Paepegem, J. Degrieck, S. Delrue, and K. Van Den Abeele, "Numerical study of the Time-of-Flight Pulsed Ultrasonic Polar Scan for the determination of the full elasticity tensor of orthotropic plates," *Composite Structures*, vol. 180, pp. 29–40, Nov. 2017.

[4] A. Martens, M. Kersemans, J. Daemen, E. Verboven, W. Van Paepegem, S. Delrue, and K. Van Den Abeele, "Characterization of the orthotropic viscoelastic tensor of composites using the Ultrasonic Polar Scan," *Composite Structures*, vol. 230, p. 111499, Dec. 2019. [Online]. Available: http://www.sciencedirect.com/science/article/pii/S0263822319311274

[5] M. Kersemans, I. De Baere, J. Degrieck, K. Van Den Abeele, L. Pyl, F. Zastavnik, H. Sol, and W. Van Paepegem, "Nondestructive damage assessment in fiber reinforced composites with the pulsed ultrasonic polar scan," *Polymer Testing*, vol. 34, pp. 85–96, Apr. 2014.

[6] M. Kersemans, A. Martens, K. Van Den Abeele, J. Degrieck, F. Zastavnik, L. Pyl, H. Sol, and W. V. Paepegem, "Detection and Localization of Delaminations in Thin Carbon Fiber Reinforced Composites with the Ultrasonic Polar Scan," *Journal of Nondestructive Evaluation*, vol. 33, no. 4, pp. 522–534, Jul. 2014.

[7] M. Kersemans, I. D. Baere, J. Degrieck, K. Van Den Abeele, L. Pyl, F. Zastavnik, H. Sol, and W. V. Paepegem, "Damage Signature of Fatigued Fabric Reinforced Plastics in the Pulsed Ultrasonic Polar Scan," *Experimental Mechanics*, vol. 54, no. 8, pp. 1467–1477, Oct. 2014.

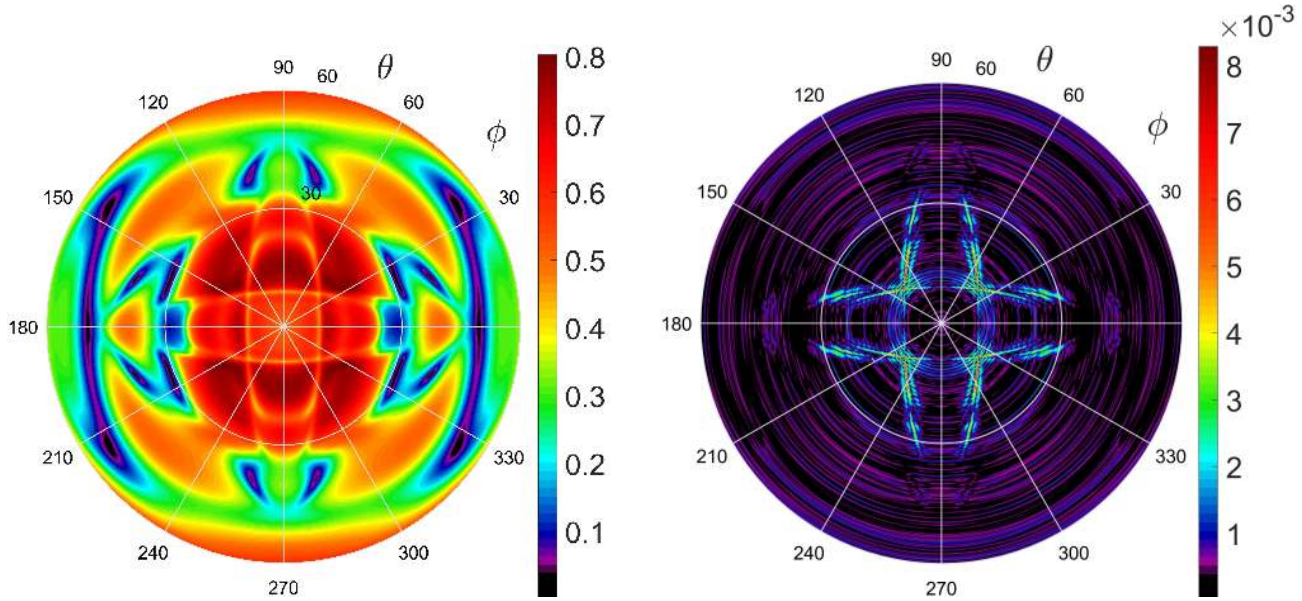

(a) (b)

Fig. 9. UPS plot of a cross-play plate of 1.25 mm thickness, using a frequency of 4.5 MHz and a good set op design parameters (a), and the absolute difference of this result with respect to the theoretical plane wave results.

[8] M. Kersemans, A. Martens, N. Lammens, K. Van Den Abeele, J. Degrieck, F. Zastavnik, L. Pyl, H. Sol, and W. V. Paepegem, "Identification of the Elastic Properties of Isotropic and Orthotropic Thin-Plate Materials with the Pulsed Ultrasonic Polar Scan," *Experimental Mechanics*, vol. 54, no. 6, pp. 1121–1132, Jul. 2014.

[9] A. H. Nayfeh, *Wave Propagation in Layered Anisotropic Media: with Application to Composites*. Elsevier, 1995, pp. 153–201.

[10] E. Verboven, M. Kersemans, A. Martens, J. Daemen, S. Delrue, K. Van Den Abeele, and W. Van Paepegem, "Matching spectroscopy with the ultrasonic polar scan for advanced ndt of composites," in *Proceedings of the 18th International Conference on Experimental Mechanics*, vol. 2, no. 8. MDPI AG, 2018. [Online]. Available: http://dx.doi.org/10.3390/icem18-05458

[11] R. Long, J. Rusell, and P. Cawley, "Non-destructive inspection of components with irregular surfaces using a conformable ultrasonic phased array," 2007, pp. 1–9.

[12] J. Daemen, A. Martens, M. Kersemans, E. Verboven, S. Delrue, W. Van Paepegem, and K. Van Den Abeele, "Numerical study of a phased array based ultrasonic polar scan to determine plane wave reflection coefficients of plates," *IEEE transactions on ultrasonics, ferroelectrics, and frequency control*, 2019.

[13] R. J. McGough, "Rapid calculations of time-harmonic nearfield pressures produced by rectangular pistons," *The Journal of the Acoustical Society of America*, vol. 115, no. 5, pp. 1934–1941, May 2004.

[14] J. A. Jensen and N. B. Svendsen, "Calculation of pressure fields from arbitrarily shaped, apodized, and excited ultrasound transducers," *IEEE Transactions on Ultrasonics, Ferroelectrics, and Frequency Control*, vol. 39, no. 2, pp. 262–267, Mar. 1992.

[15] P. Cawley and B. Hosten, "The use of large ultrasonic transducers to improve transmission coefficient measurements on viscoelastic anisotropic plates," *The Journal of the Acoustical Society of America*, vol. 101, no. 3, pp. 1373–1379, Mar. 1997. [Online]. Available: https://asa.scitation.org/doi/abs/10.1121/1.418103

[16] J. Jocker and D. Smeulders, "Minimization of finite beam effects in the determination of reflection and transmission coefficients of an elastic layer," *Ultrasonics*, vol. 46, no. 1, pp. 42–50, Mar. 2007.

Jannes Daemen was born in Kortrijk, Belgium, in 1993. He received the M.Sc. degree in Nuclear Physics from KU Leuven, Leuven, Belgium, in 2016. He is currently active as a Ph.D. student in the Wave Propagation and Signal Processing research group at KU Leuven Campus Kulak. His Ph.D. research focuses on the development of a phased array system to be used for the Ultrasonic Polar Scan, a non-destructive measurement tool to characterize composite materials.

Arvid Martens was born in Ronse, Belgium, in 1992. He received the M.Sc. degree in Soft Matter Physics from KU Leuven, Leuven, Belgium, in 2015. He is currently active as a Ph.D. student in the Wave Propagation and Signal Processing research group at KU Leuven Campus Kulak, for which received an FWO-SB research grant. During his PhD research he was also awarded an FWO travel grant and an Nvidia Seeding grant. His Ph.D. research focuses on the inverse characterization of anisotropic viscoelastic materials by means of the Ultrasonic Polar Scan, a novel non-destructive measurement tool.

Mathias Kersemans was born in 1982 in Lommel, Belgium. He has an Engineering degree in Electromechanics and in Physics. In 2014, he obtained a PhD in Applied Physics on the subject 'Ultrasonic inspection of fiber reinforced polymers'. Currently he is Professor at Ghent University, and is leading the research on non-destructive testing and evaluation of materials. His research team focuses on the development of novel inspection approaches, which includes the use of ultrasound, guided waves, active thermography, vibrometry and luminescence.

Erik Verboven was born in 1988 in Diest, Belgium. He studied Physics at KU Leuven and obtained a M.Sc. degree in 2011 and a PhD degree in 2017. The focus of his PhD research was a numerical and experimental study into the potential of using ultrasonic contrast agents for dosimetry in radiotherapy. Currently he is a postdoctoral researcher at the Department of Materials, Textiles and Chemical Engineering at Ghent University working on novel ultrasonic inspection techniques for non-destructive testing of materials.

Steven Delrue was born in Kortrijk, Belgium, in 1985. He received the M.Sc. degree in mathematics from KU Leuven, Belgium, in 2007, and the Ph.D. degree in mathematical physics and applied mathematics from KU Leuven Campus Kulak, Kortrijk, Belgium, in 2011. His Ph.D. research focused on the development of numerical models to support and optimize experimental techniques for ultrasonic non-destructive testing. Since 2011, he worked as a postdoctoral lecturer in the Wave Propagation and Signal Processing research group at KU Leuven Campus Kulak, Kortrijk, Belgium. His current research interests include the numerical modelling of contact defects and their interaction with ultrasonic waves, nonlinear signal processing techniques, ultrasonic thermography, and ultrasonic imaging using phased arrays.

Wim Van Paepegem was born in Ninove, Belgium, in 1975. He received his MSc. degree in Civil Engineering from Ghent University, Belgium in 1998. In 2002, he obtained a PhD on the subject of fatigue modelling of fibre-reinforced composites. Currently he is full professor and head of the research group Mechanics of Materials and Structures at Ghent University. His research area is focussed on experimental and computational mechanics of fibre-reinforced composites, polymers and additively manufactured materials. He is member of the Editorial Board of the journals Composites Science and Technology and Polymer Testing. He also received 5 personal awards for his scientific achievements.

Koen Van Den Abeele was born in 1965, in Lokeren, Belgium. He has a M.Sc. degree in applied mathematics from KU Leuven, Belgium, in 1987, and obtained a Ph.D. degree in mathematical physics and applied mathematics from KU Leuven, in 1992 on the subject "Alternative Fundamental Theoretical Descriptions for Acousto-optic and Acoustic Investigation of Pulsed and Profiled Ultrasound in View of Nondestructive Testing of Layered Structures". Currently he is Full Professor at the KU Leuven, head of the Wave Propagation and Signal Processing research group at KU Leuven Campus Kulak, Kortrijk, Belgium, and chair of the group Science Engineering and Technology at KU Leuven Campus Kulak, Kortrijk, Belgium. His research team focuses on theoretical modeling and experimental verification of linear and nonlinear wave propagation phenomena in liquid and solid media, and its application to non-destructive evaluation (NDE), damage detection, quality control in industrial materials, monitoring of bio(techno)logical processes, and ultrasound based dosimetry.